International Journal of Multidisciplinary Research And Studies

Available online at www.ijmras.com

INTERNATIONAL JOURNAL OF MULTIDISCIPLINARY RESEARCH AND STUDIES
ISSN: 2640 7272
Volume:07; Issue:06 (2024)
DOI: 10.5281/zenodo.11637126

Page no. 27-39

"Development, Characterization and Anti-Cancer Potential of 5-Fluorouracil Loaded Folate Appended Gellan Gum Nanoparticles for Breast Cancer Targeting"

AMIT ONKARI*[1], MEHTA PARULBEN D[2], KAJAL SHARMA[3]

[1, 2, 3] Research Scholar in Lakshmi Narain College of Pharmacy, Bhopal, (Madhya Pradesh), India

*Contact Detail: amitonkari20@gmail.com

ABSTRACT

This study explores the pharmacological investigation and anti-cancer potential of folate-modified Gellan gum nanoparticles, focusing on their impact on cancer cells through p53 activation and the inhibition of the mTOR/PI3K pathway. The nanoparticles were meticulously characterized using advanced techniques, including Nuclear Magnetic Resonance (NMR) and Fourier-Transform Infrared Spectroscopy (FTIR) to ensure structural integrity. Additionally, drug release kinetics, particle size, zeta potential, and entrapment efficiency were assessed to understand the formulation's physicochemical properties. Anti-cancer efficacy was evaluated through Sulforhodamine B (SRB) assay, demonstrating a significant reduction in cell viability upon exposure to the folate-modified Gellan gum nanoparticles. The p53 assay revealed an upregulation of the tumor suppressor protein, indicating activation of the intrinsic apoptotic pathway. Concurrently, the mTOR assay demonstrated inhibition of the mTOR/PI3K signaling pathway, further supporting the anti-cancer potential of the nanoparticles. Comprehensive characterization studies corroborated the efficacy findings, with NMR and FTIR confirming the successful modification of Gellan gum. The nanoparticle formulation exhibited controlled drug release, optimal particle size, desirable zeta potential, and high entrapment efficiency, collectively contributing to its potential as an effective anti-cancer agent. In conclusion, this research provides a thorough investigation into the anti-cancer potential of folate-modified Gellan gum nanoparticles. The synergy of SRB, p53, and mTOR assays, coupled with detailed characterization parameters, establishes a comprehensive understanding of the formulation's efficacy. These findings support the development of Gellan gum nanoparticles as a promising candidate for targeted cancer therapy, warranting further exploration and clinical translation.

Keywords: Folic Acid, Gellan Gum, P53, Mtor, SRB, Tumor Targeting, Drug Delivery

1. INTRODUCTION

1.1 Nanotechnology

Nanotechnology is science of element and fabric that cope with particle length in nanometers. The word 'Nano' is derived from Latin word, which means dwarf. Nanomedicine offers with full-size monitoring, manage, repair, defense and improve human genetic device at molecular stage the usage of engineering nanostructures and nano devices. Nanotechnology has received loads of attention with by no means-visible-before enthusiasm due to its budding capacity. It has provided satisfactory lined determination and cognizance treatment of ailment at molecular degree. Pharmaceutical nanotechnology embraces sutility of nanoscience to pharmacy as nano materials, and as gadgets like drug transport, investigative, imaging and biosensor materials. Pharmaceutical nanotechnology has furnished extra high-quality-tuned opinion and remedy of focuse dremedy of disorder at molecular degree. Nano medicine for the shipping of lively antiviral molecules by way of nanocarriers, in particular, aims at obtaining higher efficiency and slight toxicity in affected person [(1)].

Nanotechnology is the science of the small; the very small. It is the use and manipulation of matter at a tiny scale. At this size, atoms and molecules work differently, and provide a variety of surprising and interesting uses. Nanotechnology and Nanoscience studies have emerged rapidly during the past years in a broad range of product domains. It provides opportunities for the development of materials, including those for medical applications, where conventional techniques may reach their limits. Nanotechnology should not be viewed as a single technique that only affects specific areas. Although often referred to as the 'tiny science', nanotechnology does not simply mean very small structures and products [(1)].

1.2Nanoparticle

A wide range of nanocarriers are used for the delivery of anticancer drug. These include nanoparticles, nanogels, dendrimers, liposomes, and niosomes, among others. Targeted drug delivery is a method of drug administration in such a way that concentration of the drug intensifies in the diseased tissues but avoids nearby healthy tissues, which both enhance efficacy and decreasing side effects. The target zone is independent of the method and route of drug administration. Drug targeting functions at the molecular level [(3, 4)]. For effective targeted drug delivery there are four basic requirements: retention, evasion, targeting, and release. Drug targeting involves two methods frequently classified as passive and active, although these categories do not entirely define all drug-targeting strategies [(2)].

Nanoparticles are outlined as particulate dispersions or solid particles with a size within the vary of 10-1000 nm. The drug is dissolved, entrapped, encapsulated or connected to a nanoparticle matrix. Relying upon the strategy of preparation, nanoparticles, nanospheres or Nano capsules will be obtained.

The major goals in planning nanoparticles as a delivery system area unit to regulate particle size, surface properties and unharness of pharmacologically active agents so as to realize the site-specific action of the drug at the therapeutically best rate and dose plan. Chemical compound

nanoparticles offer increase the steadiness of drugs/proteins and possess helpful controlled release properties [5, 6].

1.3 Cancer

As a major cause of mortality, cancer remains a global public health concern. To date, the most common treatment of cancer has been chemotherapy, the therapeutic effect of which is far from optimal due largely to the nonspecific toxicity of chemotherapeutics. That is why the idea of cancer nanotechnology is put forward, which provides a unique approach against cancer by applying nanotechnology in cancer management [7, 8].

Compared with conventional formulations, nanocarriers possess many advantages in delivering bioactive agents either encapsulated inside the core or absorbed onto the surface: (1) Utilizing both passive and active targeting strategies, nanocarriers may guarantee the safety and efficacy of cancer treatment by changing the distribution of loaded drugs *in vivo* (i.e., increasing amount of drugs in tumor sites while minimizing the accumulation in normal tissues); (2) In light of the biodegradability, pH, ion or temperature sensibility of materials, Nano-vehicles can be functionalized to release drugs in a controlled manner**;** (3) Nano vehicles can load multiple agents based on a rational design, thereby realizing combinatorial therapy of cancer etc. [9]. Cancer is an expletive disease and became the fundamental reason for death in the recent times around the world**.** Despite the fact those decades of research and billions of funding have strengthened our understanding of the fundamental mechanisms like tumor genesis; the mortality rate caused by cancer still remains high till date [10].

2. Materials and methods

2.1 Materials

5-Fluorouracil (5-FU) was obtained as a gift sample from Neon Pharmaceuticals (MS, India). GG (Gellan gum) (Mol. Wt. 6000 Daltons) was acquired from Central Drug House (CDH), Delhi, India. Folic acid (FA) was charitably supplied by Himedia located in Mumbai, India. N-hydroxysuccinimide (NHS), dialysis membranes, 1-ethyl-3-(3- dimethylaminopropyl) carbodiimide hydrochloride (EDAC), Dicyclohexyl Carbodiimide (DCC), Pluronic F-68 were purchased from Himedia laboratories, Mumbai, India. Adipic acid dihydrazide (ADH) was purchased from Sigma Aldrich. Acetone, isopropyl alcohol and acetonitrile purchased from Merck Limited, Mumbai India and other chemicals which are consumed are of investigative chemical grade and used as brought.

2.2 Amalgamation of Folic acid-ADH-GG (FG) Copolymer

Firstly, 100 mg of FA was dispersed in 10 ml distilled water and then 500 mg of EDAC was added in FA dispersion with constant stirring, EDAC, activated the FA ends group and provide effective interaction with other group of molecules, then 500 mg of adipic acid dihydrazide was added on the activated FA dispersion and the reaction executed upto 6 hrs in room temperature. GG was dispersed in double distilled water (10ml) at 60^{o}C followed by addition of dicyclohexyl

carbodiimide (100mg) and N-hydroxysucccinimide (50mg) with constant stirring upto 12 hrs. After GG dispersion formation it was added periodically drop wise into FA-ADH solution and stirred for 6 hrs for proper and uniform interaction between amine groups of ADH and carboxyl group of GG for formation of amide bonds (carbodiimide conjugation), which shows that FA-ADH is binds with polymer (GG). The copolymer (FG) acquired was vacuum dried and authenticated by ^{1}H-NMR (Bruker DRX, USA at 400 MHz) and FTIR (IR Tracer-100, Shimadzu) spectroscopic technique.

2.3 Formation of FG nanoparticles using FA-ADH-GG Copolymer (FG) and plain polymeric nanoparticles (GG nanoparticle)

FG copolymer (10-30 mg) was dispersed in 20 ml acetone. 5-FU (30 mg) was dissipated in acetone and subsequently added drop wise into the prepared FG solution, then pluronic F-68 (250 mg) was dissolved in distilled water and various pluronic concentration (1% and 2%) were prepared. FG solution was added into pluronic solution with continuous stirring for 6 hrs. The subsequent suspension of nanoparticles was separated by membrane filter (0.45 μm) and centrifuged at 12,000 rpm for 10 min (C-24, BL, Remi, and Mumbai, India). After centrifugation discarded the supernatant and lyophilized the FG NPs for further use. Plain polymeric (GG) nanoparticles were prepared according to the method described earlier. GG NPs and FG NPs were further lyophilized and kept for upcoming studies.

2.4 Characterization parameters of FG nanoparticles and GG nanoparticles

2.4.1 Surface characteristics by Atomic force microscopy

The above mentioned AFM of the nanoparticles was done by Si micro cantilever with sample solution was spotted on mica and allowed to stand for a minute with substrate and blow off with air and observed for AFM photomicrograph by using SPM lab software.

2.4.2 Zeta potential and Particle size

The particle size and zeta potential of formulated nanoparticles is carried out by using Malvern instrument (DTS Ver. 4.10, Malvern Instruments, WR14 1XZ, UK). An appropriately diluted dispersion of GG NPs and FG was placed in the compartment of a particle size analyzer and finally average particle size and poly dispersity index were obtained.

2.4.3 DSC (Differential Scanning Calorimetry) analysis

The substantial status of nanoparticles was characterized by differential scanning calorimetry performed by utilizing DSC 60 instrument (Shimadzu, Kyoto, Japan). The samples about 10mg (FA, 5-FU, Plain FG and 5FU loaded FG NPs) were placed in the aluminum pan further the observation of DSC thermogram was observed at a scanning temperature range upto 300°C with rate of heating 10ºC/min under nitrogen atmosphere.

2.4.4 Entrapment proficiency

5-FU anchored FG NPs (10 mg) and GG NPs (10 mg) were dissipated in solvent system (acetone). Primarily, the dispersion was centrifuged at 5000 rpm (cooling centrifuge) for about 15 min, remove the polymeric debris and then supernatant was collected. The clear supernantant solution was analyzed with HPLC at 260nm wavelength, (Wasters HPLC, Model-515) to calculate the amount of loaded 5-FU in the prepared nanoparticle system [(11)].

2.4.4 *In-vitro* drug release study

Drug (5-FU) loaded FG nanoparticles and GG nanoparticles were filled in the dialysis bag (Himedia) separately and placed into separate 50 ml of phosphate buffer saline (PBS) solution at a pH 7.4 with constant stirring at 100 rpm in at 37±2°C. At a fixed time interval 1ml of buffer solution was withdrawn and replaced with the similar amount of fresh buffer solution. The amount of drug released from nanoparticles was analyzed by using HPLC system (Wasters HPLC, Model 515).

2.4.5 Hemolytic toxicity

For hemolytic activity whole human blood was amassed and collected in a collection vial as denoted in Bhadra et al (2005). Firstly human blood was centrifuged at 10,000 rpm for 10 min for complete separation of RBC and plasma. The plasma was discarded and RBC was taken for further procedure. The RBC was resuspended in saline solution to form 10% hematocrit, then the red blood corpuscles (one mL) was incubated separately with 10mL of distilled water, (taken as 100% hemolytic standard). In case of hematocrit solution with nanoparticle (drug solution), the drug loaded nanoparticle formulations was added separately on hematocrit solution (10% hematocrit) of distilled water upto 10 mL. The collection tube was allowed to stand for 1-2 hrs at 37° C, after that the drug loaded nanoparticle in hematocrit mixture was centrifuged at 5000 rpm for 5 min, then the absorbance was taken of supernatant at 540 nm to optimize the effect of nanoparticle formulations against RBCs, which was useful to predict the percentage hemolysis [(11)].

2.4.6 SRB (sulforhodamine B) assay

The 100 µl dye solution of 0.4% in 1% acetic acid was poured to each well of the plate and left in room temperature for 30 mins at followed by washing with 1% acetic acid and air dried after that 100 µl (10.5 M) of Tris buffer was added in each well and shaked with mechanical shaker for 20mins. ELISA reader was used for recording optical density of cell at 540nm wavelength.

2.4.7 mTOR Assay

The O21-404 monoclonal antibody recognizes the human mammalian target of rapmycin,(mTOR) that is phosphorylated at serine residue 2448, mTOR (pS2448). mTOR belongs to the phosphoinositide-3-kinase (PI3K)-related (PIKK) family of kinases. mTOR is also known as mechanistic target of rapamycin (serine/threonine kinase), FRAP, RAFT1, and RAPT1. mTOR functions as an amino acid and ATP sensor to balance nutrient availability and cell growth. When nutrients are sufficiently available, mTOR is activated by phosphorylation at serine residue 2448

through the PI3 kinase/Akt signaling pathway. Phosphorylated mTOR in turn activates the p70 S6 kinase and contributes to the inactivation 4E-BP1, an elF4E inhibitor. In this way, mTOR participates in the upregulation of cellular protein synthesis, growth, proliferation and survival. mTOR function may be abnormally regulated in tumors.

2.4.8 p53 expression

p53 is a 53 kD nuclear phosphoprotein that acts as a tumor suppressor protein, and is involved in inhibiting cell proliferation when DNA damage occurs. The gene for p53 is the most commonly mutated gene yet identified in human cancers. Missense mutations occur in tumors of the colon, lung, breast, ovary, bladder and several other organs. The mutant p53 is overexpressed in a variety of transformed cells and wild-type p53 forms specific complexes with several viral oncogenes including SV40 large T, E1B from adenovirus, and E6 from human papilloma virus. Wild type p53 plays a role as a checkpoint protein for DNA damage during the G1/S-phase of the cell cycle. However, it is still unclear, whether point mutated forms of p53 are simple null mutants and/or dominant negatively acting proteins.

2.4.9 Statistical analysis

Final research outcome were showed as mean ± SD. This evaluation was achieved by t-test. $P < 0.05$ was also important. All processes were performed thrice.

3. RESULTS

3.1 H-NMR and FTIR spectroscopic analysis

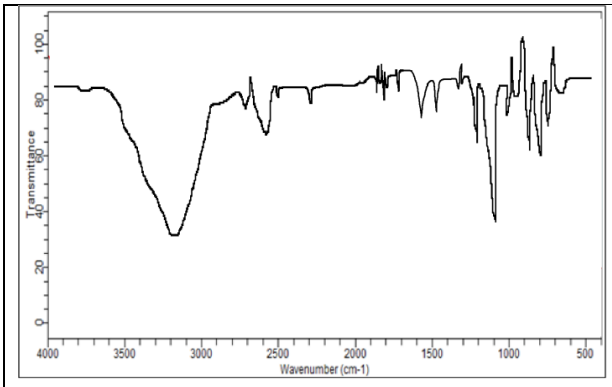

Figure: 1 FTIR spectrum of FG copolymer

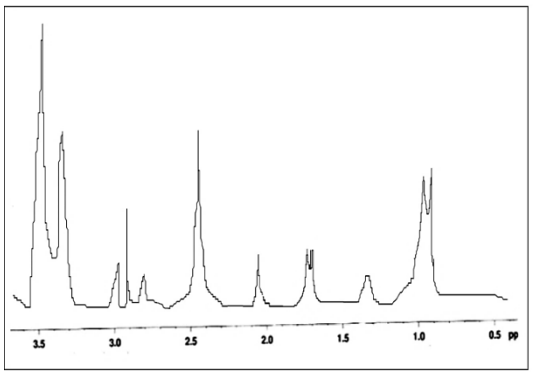

Figure: 2 NMR spectra of FG copolymer

Table: 1 Ingredients and concentration using in the formulation of FG nanoparticles.

S. No.	Drug: Polymer ratio (mg)	Internal phase			External phase		% Entrapment efficiency	Particle size (nm)
		5-FU	FG (mg)	Acetone (ml)	Pluronic	Water (ml)		

		(mg)			F-68 (mg)			
S1	30:10	30	10	20	250	25	74.50±1.50	197±1.15
S2	30:20	30	20	20	250	25	80.11±1.15	139±0.50
S3	30:30	30	30	20	250	25	93.65±1.15	84±1.10
S4	30:10	30	10	20	500	25	72.61±0.75	208±2.10
S5	30:20	30	20	20	500	25	78.32±0.75	165±1.15
S6	30:30	30	30	20	500	25	85.45±0.50	117±1.50

S: Sample, 5-FU: 5-Fluorouracil

Table: 2 Ingredients and concentration using in the formulation of GG nanoparticles.

S. No.	Drug: Polymer ratio (mg)	Internal phase			External phase		% Entrapment efficiency	Particle size (nm)
		5-FU (mg)	GG (mg)	Acetone (ml)	Pluronic F-68 (mg)	Water (ml)		
S1	30:10	30	10	20	250	25	64.25±1.50	258±0.50
S2	30:20	30	20	20	250	25	74.50±0.50	199±0.15
S3	30:30	30	30	20	250	25	90.50±1.15	105±1.50
S4	30:10	30	10	20	500	25	60.15±0.50	287±2.25
S5	30:20	30	20	20	500	25	68.21±1.75	235±1.17
S6	30:30	30	30	20	500	25	80.20±0.25	142±1.15

S: Sample, 5-FU: 5-Fluorouracil

3.2 Surface Characteristics Atomic force microscopy (AFM)

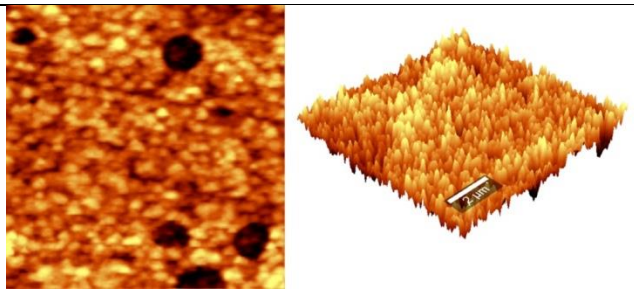

Figure: 3 AFM image of FG

Table: 3 Optimum particle size &entrapment efficiency of FG and GG nanoparticles

S. No.	Formulations	Entrapment efficiency	Particle size (nm)	Polydispersity Index	Zeta Potential
1	FG NPs	93.65±1.15	84±1.10	0.0732±0.05	-13.1 mV
2.	GG NPs	90.50±1.15	105±1.50	0.079±0.10	-5.98 mV

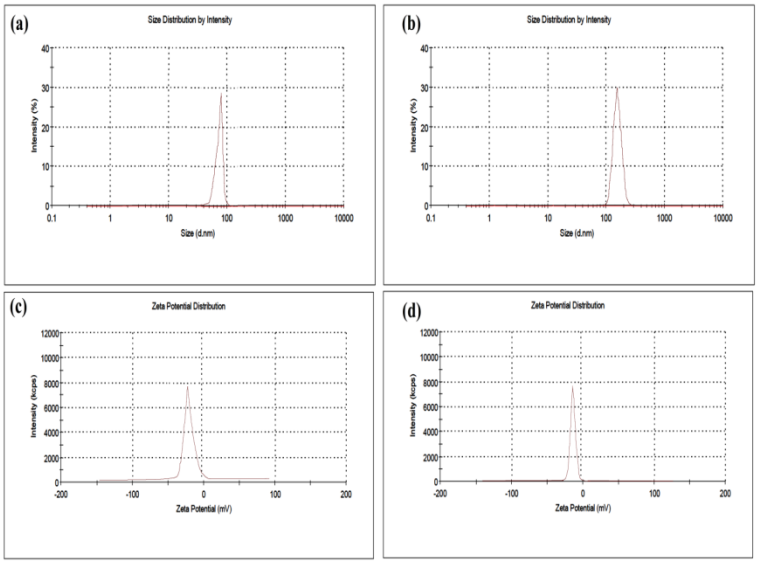

Figure :4 Particle size of (a) FG NPs; (b) GG NPs and Zeta potential of (c) FG NPs; (d) GG NPs.

3.3 Differential scanning calorimetry (DSC) analysis and *In-vitro* drug release pattern

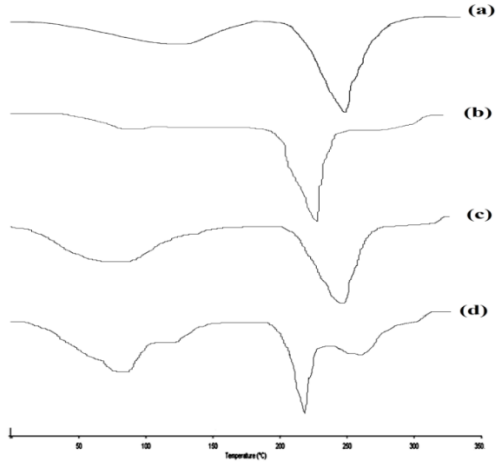

Figure: 5 DSC thermogram: (a) FA ;(b) 5-FU; (c) FG (without 5-FU); (d) FG (with 5-FU).

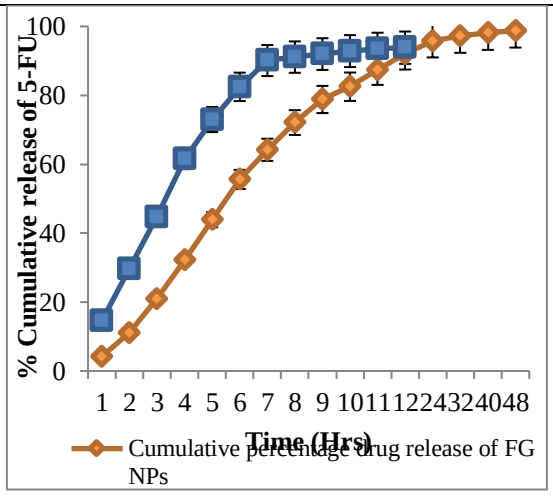

Figure: 6 Percentage cumulative 5-FU release of FG and GG NPs

3.4 HEMOLYTIC TOXICITY STUDY

Table: 4 (a) Absorbance of hemolytic standard at 540nm.

S.No.	Hemolytic Standard	Absorbance at 540nm
1	Hemolytic Standard of distilled water	0.1998

Table: 5 (b). Data of absorbance of 10% hematocrit solution at 540nm.

S. No.	10% hematocrit solution	Absorbance at 540nm	Percentage cumulative drug release
1	10% hematocrit solution of distilled water with FG NPs	0.1910	5.45%
2	10% hematocrit solution of distilled water with GG NPs	0.1825	9.15%

3.5 SRB (sulforhodamine B) assay and mTOR assay

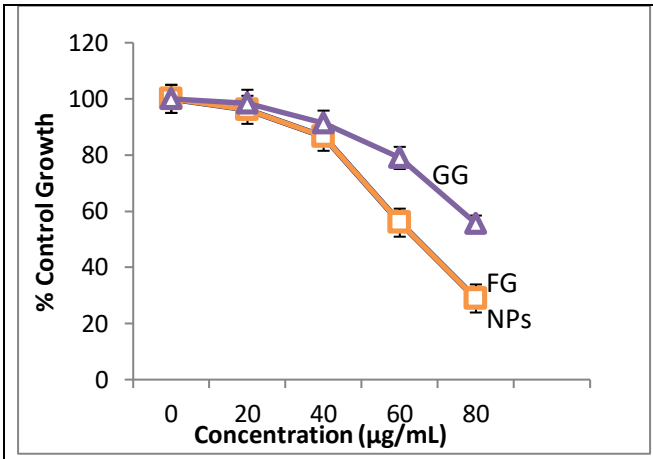

Figure : 7 *In-vitro* percentage control growth of 5-FU loaded FG NPs in MDA-MB-231 Breast Cancer cellline

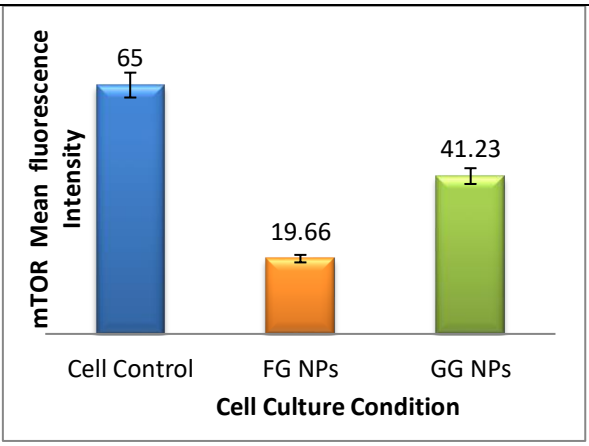

Figure: 8 The mean fluorescence intensity of mTOR-FITC against the Untreated and drug treated MDA-MB-231 human breast Cancer cells and overlay of the results plotted in Bar graph.

3.6 p53 expression

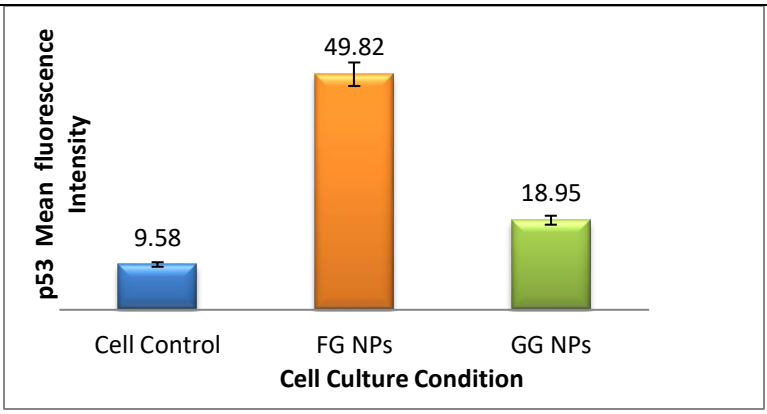

Figure: 9 the mean fluorescence intensity of p53-FITC against the Untreated and drug treated MDA-MB-231 human breast Cancer cells and overlay of the results plotted in Bar graph.

4. CONCLUSION

The 1H-NMR and FTIR spectrometers were used to validate the FG copolymer. Figure shows a spectroscopic graph of 1H-NMR and FTIR. The FTIR measurements yielded spectra ranging from 3600 cm-1 to 400 cm-1. 3250 cm-1 due to amide N-H stretch, 2750 cm-1 and 1379 cm-1 due to presence of C-H alkene bond, 1732 cm-1 due to presence of C=O stretch, 1633 cm-1 also shows C=O bond formation, 1279 cm-1 due to C-N stretching of amide bond, and 1091 cm-1 due to C=O stretching were the peaks obtained by FTIR spectra. The existence of an amide bond as well as a C=O carboxyl bond is confirmed by the appearance of characteristic peaks of 3250 cm-1 and 1633 cm-1, confirming the formation of an amide bond between the amine group of ADH and both carboxyl groups FA and GG.

Figure, shows the 1H-NMR spectra of the FG copolymer. Identical peaks in the 1H NMR spectra showed the existence of FA, adipic acid dihydrazide (ADH), GG in FG. The proton assignment of FA was 2.5 ppm, whereas the peak of GG was 1.6-2.0 ppm, and the proton assignment of adipic acid dihydrazide (ADH) was 2.6-3.0 & 3.5 ppm. The inclusion of FA, adipic acid dihydrazide, and cellulose acetate phthalate in the FG copolymer is justified by these proton assignments. To validate the conjugation as well as the compatibility of FG and cellulose acetate phthalate, a 1H-NMR and FTIR spectroscopic experiment was performed.

A method called atomic force microscopy (SPM-9500, Shimadzu) was used to assess surface properties such as form, size, and texture. As measured by AFM image single and 3D dimensions, the produced FG nanoparticles were sphere-shaped and of nanometric size range (84-208 nm). The nanoparticles are arranged uniformly and have identical heights on the photomicrograph generated from AFM analysis. The results were expected to be consistent with earlier reports.

A particle size analyzer was used to evaluate the particle size of FG nanoparticles, and the particle size of FG nanoparticles was found to be 84±1.10 nm. Because to particle aggregation, the particle size distribution ranges from 84±1.10nm to 208±2.10nm. The size of particles increases from 841.10nm to 2082.10nm nm when the quantity of cellulose acetate phthalate (GG-polymer) is increased from 10mg to 30mg, according to the results shown in Table 5.1.2. Similarly, the particle

sizes derived from GG NPs ranged from 105±1.50 to 287±2.25nm (Table 5.1.3). The PDI index of FG nanoparticles was determined to be 0.073 ± 0.05, whereas GG nanoparticles had a PDI value of 0.079 ± 0.10. The encapsulation efficiency of manufactured FG nanoparticles and GG nanoparticles was found to be 93.65±1.15% and 90.50±1.15, respectively, while the zeta potential of FG was found to be -13.1 mV and -5.98 mV for GG NPs.

The size of nanoparticles was altered by varied concentrations of surfactant and polymers, according to the results shown in the table. When the amount of GG (polymer) is increased from 10 mg to 30 mg, the size of FG particles increases from 84 nm to 208 nm, and the entrapment (drug content) efficiency decreases from 93% to 72%. This suggests that as particle size increases, the efficiency of entrapment decreases. GG nanoparticles, like FG NPs, were impacted by polymer concentration. Increasing the quantity of GG (polymer) from 10 mg to 30 mg increased the particle size from 105 nm to 287 nm. Because of the greater size of the particles and the higher quantity of polymer concentration, the entrapment effectiveness of GG nanoparticles may be lowered from 90% to 60%. The concentration of surfactant (pluronic F-68) has a major effect on particle size as well as percentage drug entrapment efficiency, and changing the concentration of surfactant from 1% to 2% may affect particle size and entrapment efficiency of FG nanoparticles. When the surfactant concentration was raised from 1% to 2%, the particle size fell and drug entrapment rose, but when the concentration was increased from 1% to 2%, the size of nanoparticles (nm) grew owing to particle gathering and the percent drug entrapped was found to be lowered. FG nanoparticles and GG nanoparticles had PDI indexes of 0.073±0.05 and 0.079±0.10, respectively. FG and GG zeta potentials were found to be -13.1 mV and -5.98 mV, respectively. The carboxyl moiety of the polymer, as well as the ligand, may be responsible for the negative zeta potential measurement of nanoparticles. Because of the greater repulsive contact, charge particles with a high zeta potential form more stable particles. The reduced negative zeta potential was shown to boost the stability of the nanoparticle system.

FA, 5-FU, FG NPs, and 5-FU loaded FG NPs, DSC thermograms were obtained and presented. At 245ºC, a minor endothermic peak was reached for FA, revealing their separate peak of FA. At 284ºC of 5-FU, an endothermic peak was obtained. FG reached an endothermic peak at 245ºC when tested without drug-loaded FG NPs. In the instance of drug-loaded nanoparticles (5-FU-FG NPs), the endothermic peak of FA was seen at 250ºC, whereas the endothermic peak of 5-FU was observed at 280- 282ºC in the nanoparticles. According to the results of DSC analysis, the exothermic peak of 5-FU was seen in the thermogram of 5-FU loaded FG NPs at 282ºC, indicating that 5-FU is present in a crystal-like state within the nanoparticle micelle.

The graph depicts the drug's sustained and extended release from a nanoparticle system. The drug release graph depicts the regulated and long-term release of 5-FU from the FG and plain polymeric (GG) nanoparticulate systems, respectively. Plain GG NPs were freed 95.15 % 5-FU in 12 hours, while FG nanoparticles were maintained 5-FU for 48 hours and released 98.52 %. This is because the solvent system used in nanoparticle carrier manufacturing, namely acetone and isopropyl alcohol, may break the FA hydrogen bond and promote the reaction of the carboxyl group of FA

and polymer GG with the amine group of adipic acid dihydrazide (carbodiimide conjugation), resulting in the formation of crosslinked core-shell micelles with lower solubility.

A hemolytic toxicity research was conducted to determine the hemotoxic impact of the designed FA anchored GG nanoparticle and plain GG NPs. Plain 5-FU, 5-FU loaded FG NPs, and 5-FU loaded GG NPs all showed hemolytic toxicity of up to 28.65±1.50%, 5.45±0.95% and 9.15±1.12%, respectively (in distilled water), Plain 5-FU and 5-FU loaded nanoparticle formulations containing 0.1μM equivalents of 5-FU. The content of medicines was used to assess the 5-FU nanoparticle formulation. Hemolytic toxicity was reduced as a result of the nanoparticls' delayed release of encapsulated drug molecules. According to the results of a hemolytic toxicity investigation, 5-FU-containing FG NPs showed less hemotoxicity than 5-FU-loaded GG NPs. This might be due to FA's hydrophilic character, which results in the hemocompatible system. Among other comparable investigations of nanoparticles published earlier, the suppression of drug hemotoxicity may be related.

The SRB test was used to establish in-vitro cytotoxicity screening of nanoparticles in the MDA-MB-231 human breast Cancer cellline. The assay's results confirm a dose-dependent evaluation of cytotoxicity, with cellular bioavailability decreasing as sample concentration increased. FG nanoparticles that have been loaded with 5-FU. Figure shows the consequence of a cell's percentage growth inhibition. Higher concentrations of 5-FU limit cell development, according to the findings. Furthermore, when the concentration of 5-FU increases, cell viability decreases. 5-FU is available in free form or encapsulated form in nanoparticles. When compared to ordinary 5-FU, NPs formulations were shown to be cytotoxic to a larger extent at concentrations between 10-80 μg/ml. The percentage growth inhibition of the cell (MDA-MB-231 human breast Cancer cells) demonstrated that greater 5-FU concentrations impede cell growth. When compared to ordinary 5-FU, NPs formulations were shown to be cytotoxic to a larger extent at concentrations between 10-80 μg/ml. In MDA-MB-231 human breast Cancer cells, the cytotoxic impact of optimized 5-FU loaded FG NPs was found to be more suppressive.

The Observation in Statistical data of mTOR expression study by flow cytometry suggesting that in MDA-MB-231 human breast Cancer cells, the expression of mTOR is high in Untreated MDA-MB-231 human breast Cancer cells (66.59 MFU) compared to the test compound (FG NPs) showing with IC50 Concentration (16 ug/ml) is showing the 19.66 MFU (mean fluoroscence intensity) of mTOR expression.

Given test compound (FG NPs) showing 19.66 of Mean Fluorescence Intensity of mTOR-PE expression with the IC50 concentration of 16ug/ml compared to the cell control which is showing 66.59 of Mean Fluorescence intensity of mTOR expression respectively. The observations suggest us that the Test compound suppressing or down regulating the mTOR expression compared to the untreated MDA-MB-231 human breast Cancer cells and the FG NPs may have possible therapeutic potential against lung cancer derived diseases.

The Observation in Statistical data of p53 expression study by flow cytometry suggesting that in MDA-MB-231 human breast Cancer cells, the expression of p53 is very low in Untreated MDA-

MB-231 human breast Cancer cells (9.58 MFU) compared to the test compound (FG NPs) showing with IC50 Concentration (16ug/ml) is showing the 49.82 MFU of p53 expression.

Given test compound (FG NPs) showing 49.82 of Mean Fluorescence Intensity of p53-FITC expression with the IC50 concentration of 16ug/ml compared to the cell control which is showing 9.58 of Mean Fluorescence intensity of p53 expression respectively. The observations suggest us that the Test compound may have possible therapeutic potential against lung cancer derived diseases.

5. REFERENCES

1) Kingsley, J. D., Dou, H., Morehead, J., Rabinow, B., Gendelman, H. E., & Destache, C. J. (2006). Nanotechnology: a focus on nanoparticles as a drug delivery system. *Journal of Neuroimmune Pharmacology*, *1*(3), 340-350.
2) Torchilin, V. P. (2000). Drug targeting. *European Journal of Pharmaceutical Sciences*, *11*, S81-S91. doi:10.1016/s0928-0987(00)00166-4
3) Gerber, D. E. (2008). Targeted therapies: a new generation of cancer treatments. Am Fam Physician.77, 311–319
4) Mimeault, M., Hauke, R., & Batra, S. (2007). Recent Advances on the Molecular Mechanisms Involved in the Drug Resistance of Cancer Cells and Novel Targeting Therapies. *Clinical Pharmacology & Therapeutics*, *83*(5), 673-691. doi:10.1038/sj.clpt.6100296
5) Vila, A., Sánchez, A., Tobío, M., Calvo, P., & Alonso, M. (2002). Design of biodegradable particles for protein delivery. *Journal of Controlled Release*, *78*(1-3), 15-24. doi:10.1016/s0168-3659(01)00486-2
6) Mu, L., & Feng, S. (2003). A novel controlled release formulation for the anticancer drug paclitaxel (Taxol®): PLGA nanoparticles containing vitamin E TPGS. *Journal of Controlled Release*, *86*(1), 33-48. doi:10.1016/s0168-3659(02)00320-6
7) Jones, D. (2007). Cancer nanotechnology: small, but heading for the big time. *Nature Reviews Drug Discovery*, *6*(3), 174-175. doi:10.1038/nrd2285
8) Saenz Del Burgo, L., Pedraz, J., & Orive, G. (2014). Advanced nanovehicles for cancer management. *Drug Discovery Today*, *19*(10), 1659-1670. doi:10.1016/j.drudis.2014.06.020
9) Misra, R., Acharya, S., & Sahoo, S. K. (2010). Cancer nanotechnology: application of nanotechnology in cancer therapy. *Drug Discovery Today*, *15*(19-20), 842-850. doi:10.1016/j.drudis.2010.08.006
10) El-Serag, H. B. (2001). Epidemiology of Hepatocellular Carcinoma. *Clinics in Liver Disease*, *5*(1), 87-107. doi:10.1016/s1089-3261(05)70155-0
11) Garg, A., Sharma, R., Pandey, V., Patel, V., & Yadav, A. K. (2017). Heparin-Tailored Biopolymeric Nanocarriers in Site-Specific Delivery: A Systematic Review. *Critical Reviews™ in Therapeutic Drug Carrier Systems*, *34*(1), 1-33. doi:10.1615/critrevtherdrugcarriersyst.2017016794